

Electronic structure and magnetism of Ni overlayers on a Cu(001) substrate

Ding-sheng Wang*

Physics Department, Northwestern University, Evanston, Illinois 60201

A. J. Freeman

*Physics Department, Northwestern University, Evanston, Illinois 60201**and Argonne National Laboratory, Argonne, Illinois 60439*

H. Krakauer

Physics Department, College of William and Mary, Williamsburg, Virginia 23185

(Received 28 January 1982)

Our recently developed linearized augmented-plane-wave thin-film method is used to determine the electronic structure and magnetism of Ni overlayers on Cu(001). Accurate *ab initio* self-consistent spin-polarized semirelativistic band calculations are reported for (i) a clean five-layer Cu(001) slab and (ii) the same Cu slab plus one or two $p(1 \times 1)$ layers of Ni on either side. Results presented include charge and spin densities, work function, band structures, projected density of states, magnetic moments, and direct and transferred hyperfine fields. Both surface and interface effects are found to be important. The Ni overlayers are not magnetically dead: The Ni layer adjacent to the Cu has its moment *decreased* from the bulk value to $0.39\mu_B$ for the single Ni overlayer and to $0.47\mu_B$ for the two-Ni-thick layers; the surface Ni layer in the two-layer Ni on Cu film has its moment *increased* somewhat to $0.68\mu_B$. This reduction in moment for the interface Ni arises primarily from charge transfer onto Ni sites from the Cu substrate. By contrast, the increase in moment of the Ni surface atoms arises in large part due to the dehybridization of the p electrons from the d -band electrons; these p electrons become more delocalized and spill out into the vacuum region. A similar effect was also observed for an unsupported Ni monolayer. In the case of the Ni monolayer on Cu, the total number of Ni electrons is almost the same as for bulk Ni. Here, the loss of electrons due to the dehybridization of p electrons is nearly canceled by the increase from its interface with the Cu substrate; the decrease in magnetic moment (to $0.39\mu_B$) agrees with electron-capture experiments.

I. INTRODUCTION

The unique chemical and physical properties of the transition metals and their alloys and compounds have made them prime candidates for experimental and theoretical studies. Recently, this interest has focused on achieving a better understanding of the properties of transition-metal materials on the microstructure scale, such as super-fine particles, surfaces, interfaces, and modulated structures. One of the most interesting of these is the nature of surface magnetism—a problem which has attracted a great deal of interest since the first reports¹ of the existence of a magnetically “dead” layer on the Ni surface. To date, experiments have been made on many materials (Fe, Co, Ni, and alloys) in different forms,^{2–4} but have yielded inconclusive results. Discrepancies between the different

results have been attributed partly to the difficulties of preparing a perfect clean surface, and partly to the difficulties of interpreting results obtained from probing only a few atomic layers. For example, in the case of pure Ni, electron capture³ showed no dead layers, whereas polarized neutron scattering⁴ on small Ni particles confirmed its existence. Other experiments have been made on atomic overlayers of magnetic metals deposited on nonmagnetic substrates—an approach which has some apparent advantages such as a simplification of some measurements and the use of the overlayer thickness as a (controllable) parameter. The Ni overlayer on a Cu substrate is the most widely studied system. Because of the good match between their fcc lattice constants ($a_{\text{Ni}} = 3.524 \text{ \AA}$ which is close to $a_{\text{Cu}} = 3.615 \text{ \AA}$) and the close resemblance of many of their properties, a near to

ideal overlayer structure is expected for this system. Anomalous Hall-effect measurements by Bergmann⁵ confirmed¹ the existence of a dead layer of Ni on Cu when the Ni overlayer is less than about 2.5 atomic layers. However, Pierce, *et al.*⁶ concluded from the spin polarization of photoemitted electrons that ferromagnetism occurs when the Ni overlayer is only one to two atomic layers thick. More recently, electron-capture spectroscopy measurements by Rau⁷ showed that even a monolayer of Ni on Cu(001) substrate is magnetic, but with a reduced magnetic moment.

On the theoretical side, although some earlier models^{8,9} showed that the surface layers of a ferromagnetic crystal such as Ni may be magnetically "dead," linear combination of atomic orbital (LCAO), self-consistent calculations by Wang and Freeman,¹⁰ and linearized augmented-plane-wave (LAPW) calculations by Jepsen *et al.*¹¹ showed that the Ni(001) surface is not magnetically "dead" but has instead a moment comparable to that of the bulk. The work reported in Ref. 10 gives a 20% decrease of the magnetic moment ($0.44\mu_B$) compared to $0.54\mu_B$ obtained for the center layer of their nine-layer film, whereas Ref. 11 shows essentially no change in magnetic moment for the surface layer ($0.61\mu_B$, compared to $0.58\mu_B$ for the center layer) for a five-layer film. A more recent calculation,¹² also on a thin five-layer Ni(001) film using the method described in Sec. II, shows a 15% increase of the moment of the surface atom of Ni(001) films, from $0.62\mu_B$ for the center layer to $0.72\mu_B$ for the surface. A similar increase has also been obtained for the surface magnetism of a five-layer Ni(110) film.¹²

In bulk Ni, the theoretical exchange splitting is about 0.6 eV, the majority (spin-up) $3d$ band is fully occupied, but with its upper edge only ~ 0.3 eV below the Fermi energy (E_F), and its minority hole states quite close to E_F . As a result, the magnetic properties of the surface Ni atoms are vulnerable experimentally to surface contamination¹³ or theoretically to a number of factors which may influence by ~ 0.3 eV any surface states or bulk states in the d bands. Certainly the charge transfer near the surface region, or the change of the bonding of the surface atoms with its neighbors, gives rise to the change of the energy of some states. The challenge to theoretical treatments of the problem of surface magnetism is to handle these states with an accuracy of better than 0.1 eV.

In this paper we report results of the first determination¹⁴⁻¹⁶ of the electronic structure and

magnetism of Ni overlayers of Cu(001). We use our recently developed LAPW thin-film method^{17,18} to carry out accurate self-consistent spin-polarized semirelativistic energy-band calculations on Ni overlayers on a Cu(001) substrate, consisting of a five-layer Cu(001) slab plus one or two $p(1 \times 1)$ layers of Ni on either side, referred to as Ni-Cu and 2Ni-Cu, respectively. As in the case of the Ni-Cu results reported briefly earlier,¹⁶ we find that the Ni overlayers are not magnetically dead. The Ni layer adjacent to the Cu has its moment decreased to $0.39\mu_B$ for Ni-Cu and to $0.47\mu_B$ for 2Ni-Cu, whereas the surface Ni layer in the 2Ni-Cu film has its moment increased to $0.68\mu_B$ compared to $0.62\mu_B$ at the center of a five-layer Ni(110) film.¹² This reduction in moment for the interface Ni arises primarily from charge transfer onto these Ni sites from the Cu substrate. By contrast, the increase in moment of the Ni surface atoms arises in large part due to the dehybridization of the p electrons from the d -band electrons. These p electrons become more delocalized and spill out into the vacuum region. A similar effect was observed for an unsupported Ni monolayer.¹² In the case of a monolayer of Ni on Cu, the total number of Ni electrons is closer to that of bulk Ni (the loss of electrons due to dehybridization of p electrons is partially canceled by the increase from its interface with the Cu substrate), but the magnetic moment $0.39\mu_B$ decreases about 40%—in agreement with electron-capture experiments.⁷ This decrease is also connected with the majority hole formed from the surface state above the Ni $3d$ band edge near \bar{M} .

II. METHODOLOGY

We employ the self-consistent LAPW film method^{17,18} as generalized to deal with spin polarization. The spin-dependent exchange-correlation potential V_{xc} of von Barth and Hedin¹⁹ is used in the local spin-density-functional formalism to determine the electronic energy-band structure,

$$V_{xc}^{\alpha} = A(\rho)(2\rho^{\alpha}/\rho)^{1/3} + B(\rho), \quad (1)$$

where $\rho^{\alpha} = \rho^{\uparrow}$ or ρ^{\downarrow} , and $\rho = \rho^{\uparrow} + \rho^{\downarrow}$ denote the spin-up or spin-down and the total electron density, respectively. The A and B coefficients are given by¹⁹

$$A(\rho) = \mu_x^2(\rho) + v_c(\rho),$$

$$B(\rho) = \mu_c^2(\rho) - v_c(\rho),$$

where

$$\mu_x^p(\rho) = -(3/\pi)^{1/3} \rho^{1/3}$$

and

$$\mu_c^p(\rho) = -c^p \ln[1 + (4\pi/3)^{1/3} r^p \rho^{1/3}]$$

are the contribution of exchange and correlation to the chemical potential, and

$$v_c(\rho) = -\frac{4}{3} \frac{1}{2^{1/3}-1} \left[c^f F \left(\frac{1}{(4\pi/3)^{1/3} r^f \rho^{1/3}} \right) - c^p F \left(\frac{1}{(4\pi/3)^{1/3} r^p \rho^{1/3}} \right) \right],$$

with the function

$$F(z) \equiv (1+z^3) \ln(1+1/z) + z/2 - z^2 - \frac{1}{3}.$$

The coefficients c^f and r^f are set equal to $c^p/2$ and $2^{4/3} r^p$, respectively, according to scaling suggested by the random-phase approximation,¹⁹ and $c^p=0.0225$ and $r^p=21.0$ are chosen to yield the paramagnetic correlation term of Hedin and Lundqvist.²⁰

The core charge density ($1s^2 2s^2 2p^6 3s^2 3p^6$) is computed using a fully relativistic Dirac-Slater-type atomic-structure program, while for the valence electrons only a semirelativistic computation (without spin-orbit coupling) is used. All states, including the core states, are computed self-consistently for every iteration. This is important for the calculation of the hyperfine field because the core-polarization Fermi-contact part is the dominant contribution.

In the interstitial and vacuum regions, the full potential without the shape approximation is determined self-consistently and included in the computations while nonspherical terms are neglected inside the muffin-tin spheres. The Coulomb potential is obtained by a very accurate solution of Poisson's equation¹⁸ permitting a very precise determination of the potential near the surface region and thus gives a good description of the surface states and surface electronic properties.

The structure of the Cu(001) five-layer slab used as substrate to the Ni overlayers, is the ideal one, i.e., that obtained from a bulk Cu crystal without any relaxation or reconstruction. Thus, the 2D periodicity of the Ni overlayer is assumed identical to that of the Cu substrate. The z distance between the Ni and interface Cu layer is set equal to 1.81 Å to agree with the bulk Cu lattice interlayer spacing. For the 2Ni-Cu film the z distance between the surface and interface Ni layer is set

equal to that of bulk Ni (1.76 Å). Because of the relatively good match between Cu and Ni lattice parameters, this choice of structural parameters seems quite reasonable, and is not expected to affect greatly the physical results obtained.

For the Ni-Cu system under consideration (seven atoms per unit cell), the basis size of over 190 LAPW's per z -reflection symmetry type (55 LAPW's per atom) results in eigenvalues which are converged to better than 3 mRy. For 2Ni-Cu (nine atoms per unit cell), the basis size of about 210 LAPW's per z -reflection symmetry type (47 LAPW's per atom) yields a convergence of the d -state eigenvalues to about 5 mRy. 15 \bar{k} points in the $\frac{1}{8}$ irreducible wedge of the 2D Brillouin zone (BZ) are used to generate the charge density in the self-consistency process. We consider self-consistency achieved when the rms difference between input and output potential is less than 15 mRy. The self-consistent process for the spin-polarized case starts from a well-converged paramagnetic self-consistent potential. A magnetic field (~ 2 mRy) is switched on in the first iteration to generate a magnetized state and then it is switched off for all succeeding iterations. The magnetic moments of the Ni atoms are observed to increase from about $0.1\mu_B$ for the first iteration to its converged value, while the moments on the Cu atoms decrease to essentially zero. The magnetic moments are found to converge more quickly in the iteration procedure than does the potential. For the clean Cu five-layer film (which is used as comparison), the convergence and self-consistency are much better, e.g., the difference between the input and output potential is less than 4 mRy.

III. ELECTRON DENSITY AND WORK FUNCTION

The theoretical self-consistent total electron density of the 2Ni-Cu film is shown in the contour plot [Fig. 1(a)] on a vertical cut plane passing through a line connecting a surface atom with one of its nearest neighbors in the second layer. (A similar result for the Ni-Cu case was presented earlier.¹⁶) Outside the surface layer, the electron density decreases exponentially toward the vacuum, with some strong curvature in the contours near the surface in keeping with the atomic nature of the surface layer. From just below the surface layer, the electron distribution is almost identical with that of the center layer, which is then assumed to approximate the bulk. No large differ-

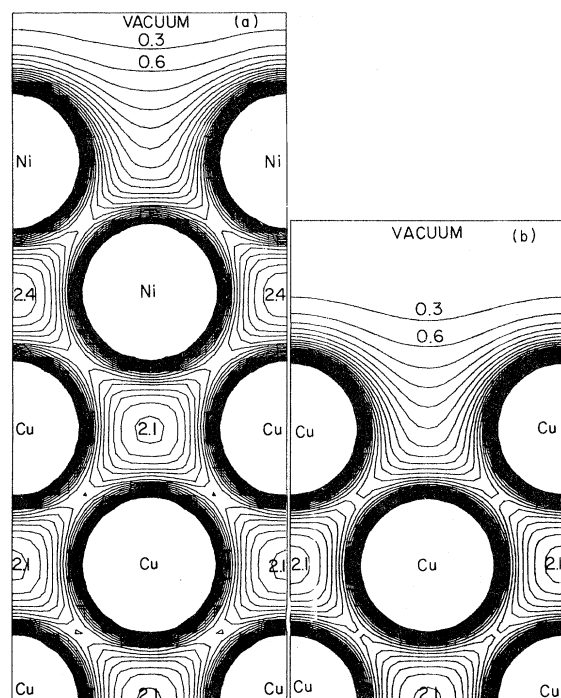


FIG. 1. Self-consistent total charge density of (a) a nine-layer film consisting of a Cu(001) five-layer substrate covered with a two-layer Ni film on each side and (b) a clean five-layer Cu(001) film. The contour plot shown is on a vertical-cut plane passing through a line connecting a surface atom with one of its nearest neighbors in the second plane of atoms. Each unit is 0.01 a.u.

ences can be seen in the interstitial region of the Ni interface, Cu interface, and the inner Cu layers. Comparison of these results with that of the clean Cu surface given in Fig. 1(b) shows that the conduction-electron distribution at the surface of the clean Cu film is almost the same as that of the Ni surface layer of 2Ni-Cu. This result is not surprising because the main contribution in this region, as shown by the contours in Figs. 1(a) and 1(b), comes from the 4s electrons which are not very different for Ni and Cu. It serves to emphasize that the well-known large differences in the chemical and physical properties between the Ni and Cu surfaces must be due to their 3d bands (which contribute to the high electron density in the region closer to the atom centers).

Table I gives the total number of valence electrons inside the touching muffin-tin spheres for the three film systems studied. The bulk value given in the right column is obtained from the center layer of a five-layer pure Ni film by the same method.¹² The effect of the surface is seen from

TABLE I. Total number of the valence electrons inside touching muffin-tin spheres (the radii are 2.354 a.u. for bulk Ni, 2.385 a.u. for the surface Ni layer of 2Ni-Cu, and 2.415 a.u. for all the other Ni and Cu spheres). The order of the layers as shown in the left-hand column is from the surface (top) to the center (bottom) in each of the slabs.

	2Ni-Cu	Ni-Cu	Cu	Bulk Ni ^a
Ni	9.06			9.22
Ni	9.37	9.21		
Cu	10.38	10.35	10.21	
Cu	10.38	10.37	10.37	
Cu	10.38	10.39	10.38	

^aLAPW bulklike value: center layer of a Ni(110) five-layer film (Ref. 12).

the decrease of the number of electrons belonging to the surface atom. For example, the number of electrons in the surface atom of the clean Cu five-layer film is ~ 0.17 less than that at the center, and the surface Ni layer of the 2Ni-Cu film is also ~ 0.17 less than the bulk value. However, in sharp contrast, the interface Ni layer atoms in contact with the Cu substrate have 0.15 *more* electrons than in the bulk. For the monolayer of Ni on Cu substrate, both effects cancel each other, and leave the total number of valence electrons of this layer almost unchanged as compared to the bulk.

An orbital decomposition of the valence electrons (Table II) gives more information of this change due to the surface and interface effect. The decrease of the *s*-like component of the Ni(*S*) atom is obviously due to the expansion of the extended 4*s*-like state toward the vacuum in an attempt to lower its kinetic energy. The *p*-like component of the electron density in the muffin-tin region of the surface atom is markedly reduced compared to that at the Ni(*I*) atom; this reduction is approximately proportional to their coordination number. The decrease of this *p*-like component for the surface layer, which may be caused by the mixing with the *s*-tails of neighboring atoms, is due largely to dehybridization with the *d* electrons. For the clean Cu five-layer film, the *s*-, *p*-, and *d*-like components are also given in Table II. The center and surface layers and a similar dehybridization effect seen here. The change of this *p*-like component is the dominant part of the change seen in the total change given in Table II for Ni(*S*) and Ni(*I*). The difference in *d*-like and *s*-like components in Ni(*S*) and Ni(*I*) is much less pronounced.

Starting from very different initial potentials, independent self-consistent calculations were carried

TABLE II. Orbital decomposition of the total number of valence electrons inside touching muffin-tin spheres of double-layers of Ni on Cu(001) substrate and a clean Cu(001) film. S , I , $I-1$, and C in the first column denote the surface, interface, subinterface, and center layer, respectively.

		s	p	d	Total
2Ni-Cu	Ni(S)	0.432	0.268	8.341	9.06
	Ni(I)	0.478	0.433	8.416	9.37
	Cu(I)	0.535	0.470	9.335	10.38
	Cu($I-1$)	0.535	0.456	9.341	10.38
	Cu(C)	0.536	0.464	9.345	10.38
Cu	Cu(S)	0.520	0.317	9.348	10.21
	Cu($S-1$)	0.529	0.467	9.337	10.37
	Cu(C)	0.528	0.475	9.338	10.38

out for the three film systems studied here. As can be seen from Table I, the degree of consistency of the final results for the Cu layers is very impressive. For example, the difference in the number of electrons of the two innermost Cu layers for all three systems is within 0.02 electrons. This not only indicates that the results are stable with respect to film thickness, but it also gives an estimate of the precision of the calculation, which is determined by the number of LAPW's used and the self-consistency achieved in the calculation. In fact, 0.02 electrons inside the muffin-tin region give a Coulomb contribution of about 17 mRy at the boundary ($r=2.42$ a.u.), consistent with the degree of self-consistency of the potential achieved.

As is well known, a good check of these film calculations is a comparison of the calculated work function W with experiment. The work function is very sensitive to the charge transfer due to the surface effect, and depends especially on charge transfer in the z direction. The results are 4.94, 5.45, and 6.10 eV for clean Cu, Ni-Cu, and 2Ni-Cu, respectively. There are no published data for the Ni on Cu system to our knowledge. Electron transfer at both the free surface (Ni to vacuum) and interface (Cu to Ni) is expected to increase the work function. The value of W for the clean Cu film is in good agreement with experiment²¹ and an earlier self-consistent LCAO calculation.²²

Our calculations also yield a chemical shift for the $3p_{3/2}$ core level of the surface atoms (Table III) in keeping with the expectation that these core states shift to reduced binding energy as predicted by a simple model²³ for core-level shifts in d -band metals. Since Cu has more than half-filled d bands, this model predicts a shift to reduced binding energy. The result for clean Cu, 0.60-eV shift, is consistent with the result for Cu(111) obtained

by Appelbaum and Hamann.²⁴ However, this shift has not been observed in XPS experiments on either Cu (Ref. 25) or Ni (Ref. 26) [although it has been observed in Au (Ref. 23)].

Since this is the first calculation of a Ni on Cu system, we first compare our results instead with other theoretical calculations on clean Ni or clean Cu films. The charge-density contour plots in Fig. 1 are in good agreement with the LCAO calculation on the clean Cu film (Fig. 10 in Ref. 22). The decrease in the number of electrons of the surface atoms (0.18) found in another LAPW calculation¹¹ on a clean Ni film is consistent with our results, namely, 0.17 for clean Cu and 0.16 for the Ni surface of 2Ni-Cu compared with bulk Ni. These results mean, at least for the charge transfer along the z direction, that different methods give a rather good consistent description of the surface effect. The orbital decomposition given in Table II shows that the number of p -like electrons is in agreement with LAPW results by Jepsen *et al.*¹¹ and Krakauer and Freeman¹² for the clean Ni(001) film.

TABLE III. $3p_{3/2}$ core levels of 2Ni-Cu, Ni-Cu, and clean Cu(001) films (in eV) with $E_F=0$. The average of the spin-up and spin-down state is shown. The splitting due to the spin polarization is shown in parentheses for Ni atoms. For Cu atoms, it is essentially zero (<0.003 eV).

	2Ni-Cu	Ni-Cu	Cu
Ni	-61.90 (0.75)		
Ni	-62.16 (0.53)	-61.74 (0.42)	
Cu	-68.69	-68.57	-68.15
Cu	-68.79	-68.69	-68.65
Cu	-68.76	-68.73	-68.75

IV. ENERGY BANDS: SURFACE AND INTERFACE EFFECTS

The layered projected densities of states (DOS) of the Ni-Cu film are plotted in Fig. 2, with the results for the clean five-layer Cu(001) film also shown for comparison. The DOS of the center Cu layer is unchanged when the clean Cu film is covered with the Ni overlayers. Even the subinterface layer Cu($I-1$), which is the next-nearest neighbor of the Ni overlayer, has almost the same DOS as that of a clean Cu film. This finding is consistent with the electron-density result (Fig. 1) that right from the second layer, the electron distribution is the same as in the bulk; it also indicates that the Cu five-layer film is a thick enough substrate for undertaking a study of the properties of the Ni overlayer.

A large effect of covering Cu with the Ni overlayer is observed only for the outermost Cu layer which is in direct contact with the Ni layer. Firstly, the surface narrowing of the surface DOS of the clean Cu film disappears with this monolayer coverage. The DOS curve of this Cu(I) layer of the Ni-Cu film becomes similar to that of other interior Cu layers. Secondly, the upper edge of the outermost Cu $3d$ bands moves 0.2 eV to greater binding energy after coverage, indicating that in clean Cu the d bands of the surface layer have moved 0.2 eV to reduced binding energy. This effect can also be seen by comparing the DOS of the surface and the center layer of the clean five-layer film.²²

The same phenomena occur in the 2Ni-Cu system as seen in Fig. 2 for Ni-Cu. Upon coverage of a second Ni surface layer, the width of the local DOS curve of the inner Ni layer, Ni(I), increases to 2.7 full width at half maximum (FWHM) from 1.6 eV for the Ni layer of the Ni-Cu system due to the increase of the DOS at higher binding energy corresponding to the Ni-Cu interface bonds. The upper edge of the DOS of the surface of 2Ni-Cu is 0.2 eV above the interface layer. These changes in the $3d$ bands due to the surface interface effects influence the filling of the electrons in the Ni $3d$ bands because of the high DOS at E_F , and then affect the magnetic properties of the surface and interface layers.

The energy bands of the Ni-Cu film are plotted in Fig. 3. The Ni states (defined as those having more than 60% of their charge in the surface layer) are marked by the solid circles. For bulk crystalline Ni, at the Γ point of the 3D Brillouin zone ($\vec{k}=0$), the spin-up t_{2g} state is at about -2.3

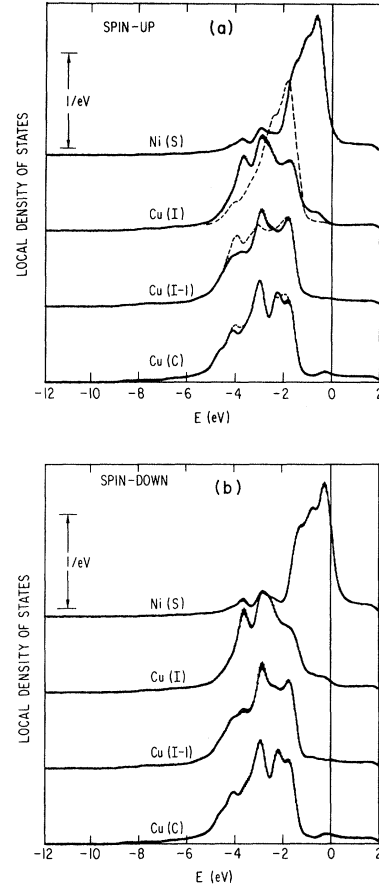


FIG. 2. Spin-polarized layer projected density of states of a five-layer Cu(001) slab covered with a $p(1 \times 1)$ monolayer of Ni on each side: (a) spin-up, (b) spin-down. S, I, I-1, and C denote the surface, interface, subinterface, and center layers. The dashed lines show the results of a clean five-layer Cu(001) film.

eV with respect to E_F .^{27,28} For the Ni overlayer on Cu, the $d_{x^2-y^2}$ orbit²⁹ [$\bar{\Gamma}_3$ in Fig. 3(a)] which is directed to the nearest-neighbor Ni atoms in the same layer, has nearly the same energy, but the doublet $d_{xz,yz}$ [$\bar{\Gamma}_5$ in Fig. 3(a)] which is directed to the atoms in the neighboring layers, is raised by 1.6 eV to reduced binding energy due to the removal of its neighbors from outside the surface. Similarly, the d_{xy} orbital [$\bar{\Gamma}_4$ in Fig. 3(a)] is shifted about 1.0 eV to reduced energy. This is why the upper edge of the d band moves to the reduced binding energy.

At \bar{M} all the Ni $3d$ states in the Ni-Cu film are well localized at the surface. The layer-by-layer electron energy and symmetry properties of all the \bar{M} states (spin-up) are shown in Fig. 4. The right-hand panel of Fig. 4 shows the corresponding result of an isolated Ni monolayer.¹⁶ The Ni $d_{x^2-y^2}$

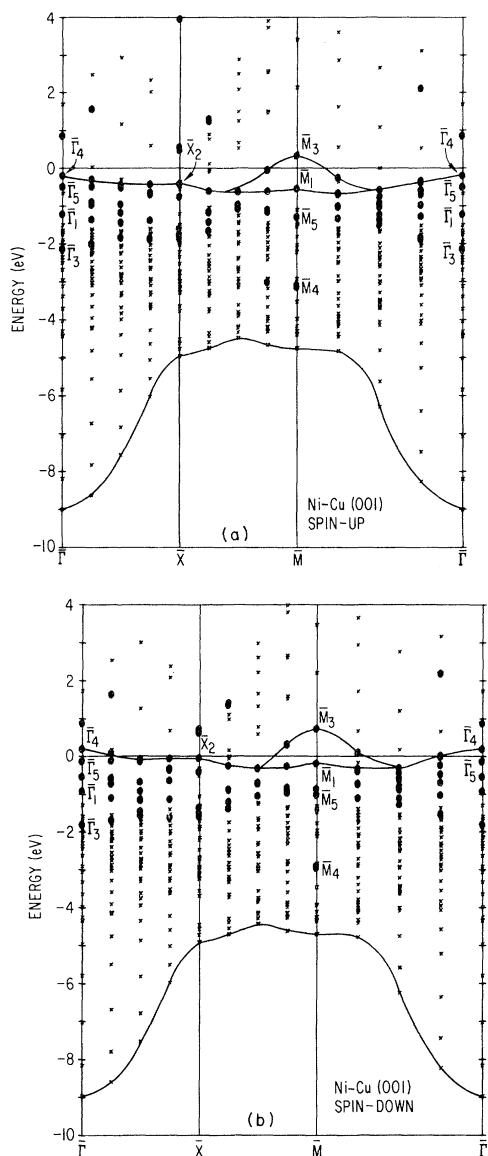


FIG. 3. Band structure of a five-layer Cu(001) slab covered with a $p(1 \times 1)$ monolayer of Ni on each side: (a) spin-up, (b) spin-down. Solid circles denote states with more than 60% of electrons in the surface Ni overlayer.

orbital, which does not mix with other states for symmetry reasons, constitutes a surface band [\bar{M}_3 in Fig. 3(a)] above the d -band edge. It is similar in nature to the surface states reported for the clean Cu(001) film^{17,22} and observed in photoemission experiments,³⁰ and similar to that of the clean Ni(001) film.^{10,17} As in the case of the clean Ni film, this spin-up \bar{M}_3 state lies above E_F for the surface Ni layer in either the Ni-Cu or the 2Ni-Cu films, so a pocket of majority holes forms and reduces the surface magnetism.

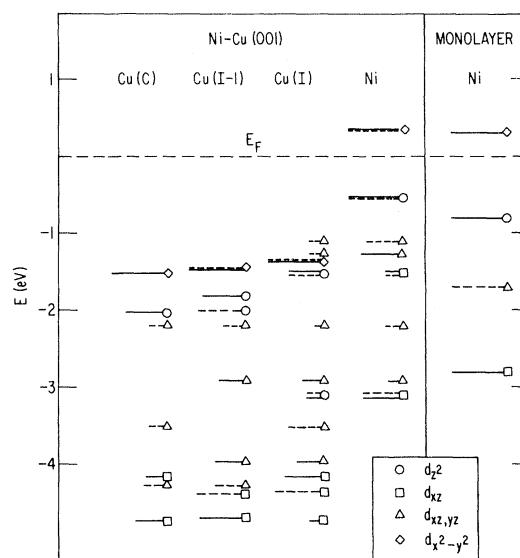


FIG. 4. Energy and symmetry of the majority states of \bar{M} of a five-layer Cu(001) slab covered with a $p(1 \times 1)$ monolayer of Ni on each side. The horizontal length of the bars gives the layer-projection coefficient of the state in the specified layer (some are omitted when they are too small). The mixing of the wave function of the states of many layers is represented by the bars of one eigenstate on corresponding layers. Dashed lines represent the states antisymmetric with respect to the z reflection. The different symbols beside the bars represent d_{z^2} , d_{xy} , $d_{xz,yz}$, and $d_{x^2-y^2}$ states, respectively. Corresponding results of an isolated monolayer Ni film are also shown for comparison, but with its Fermi energy aligned to that of the Ni-Cu film.

At \bar{M} the d_{z^2} orbital of the Ni atom does not mix with the substrate states either, because a symmetry allowed state, such as d_{xy} of the interface Cu layer, is about 4.5 eV away. The splitting in energy between the Ni $3d_{x^2-y^2}$ and $3d_{xy}$ orbitals at \bar{M} increases from the bulk value due to the presence of the surface.³¹ (For the isolated Ni monolayer, this difference in energy is 1.22 eV. Here, the strongest "surface" perturbation is expected.) For the Ni surface layer, this difference is 0.87 eV for the Ni-Cu, and 0.76 eV for the 2Ni-Cu system. When the Ni layer is totally covered, as in the interface Ni layer of the 2Ni-Cu film, it is only 0.37 eV—about the same as for the interior Cu layer—indicating that there is little surface perturbation in this case. This change should arise mainly from crystal-field effects because both states, especially the Ni $d_{x^2-y^2}$ and d_{z^2} states, do not mix with other states.

By contrast, rather strong mixing with the sub-

strate states at \bar{M} occurs for the Ni $d_{xz,yz}$ and d_{xy} states. The Ni $d_{xz,yz}$ state has been pushed slightly higher in energy by the mixing, as can be seen by comparing the same state of the Ni on Cu substrate and the isolated Ni monolayer film in Fig. 4. It is above the substrate bulk band with the same symmetry, and is then a surface state localized near the surface. The Ni d_{xy} state mixes strongly with the d_{z^2} state of the interface Cu atom because they lie close in energy, and pushes the interface Cu d_{z^2} state slightly higher and the Ni d_{xy} state slightly lower in energy (Fig. 4).

V. SURFACE AND INTERFACE EFFECTS ON THE MAGNETIZATION

The spatial distribution of the spin density, plotted in Fig. 5 for the 2Ni-Cu film, shows that the magnetization is localized in the Ni layers. The magnetization is essentially zero on the Cu layers; the few contours shown in Fig. 5 close to the Cu nucleus are due mainly to the noise in the computation. The vacuum and interstitial regions are slightly polarized in the opposite direction, similar to that reported for the clean Ni(001) film.¹⁰ The layer-by-layer magnetic moments (contributed by

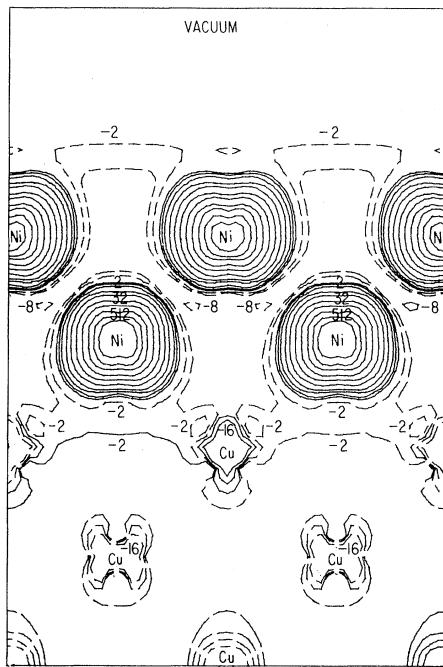


FIG. 5. Contour plot of the spin density of a five-layer Cu(001) slab covered with a two-layer Ni film on each side. Each unit is 0.0001 a.u. with successive contours given in a ratio of 2.

TABLE IV. Magnetic moment μ inside the muffin-tin spheres of the 2Ni-Cu and Ni-Cu film, in Bohr magnetons. The order of the layers as shown in the left column is from the surface (top) to the center (bottom).

	2Ni-Cu	Ni-Cu	Bulk Ni ^a
Ni	0.68		0.62
Ni	0.47	0.39	
Cu	-0.02	0.00	
Cu	0.00	0.00	
Cu	-0.01	0.00	

^aLAPW bulklike value: center of layer of a Ni(110) five-layer film (Ref. 12).

the electrons inside the touching muffin-tin spheres) are listed in Table IV. The magnetic moment of the surface Ni layer of the 2Ni-Cu film increases by about 10% to $0.68\mu_B$ compared to the bulk value $0.62\mu_B$ calculated by the same method.¹² The moment of the interface layer Ni(I) of the 2Ni-Cu film decreases by 24%, and the Ni layer of the Ni-Cu system decreases by 37% compared to the calculated bulk value. The orbital angular-momentum decomposition of the layer-by-layer contribution to the magnetic moment is given in Table V. It is seen that the contribution to the moments arises almost completely from the d -like component, similar to that in the clean Ni film.¹¹ Examination of Table V reveals that this correlation is actually with the number of p -like electrons which show the largest change in occupancy.

As shown in Fig. 6(a), a good linear relation is observed between the magnetic moment and the total number of electrons inside the touching muffin-tin spheres for all the Ni layers including the 2Ni-Cu, the Ni-Cu, the isolated monolayer of Ni,¹⁶ and the clean Ni(100) and Ni(110) (Ref. 12) film. The magnetic moment decreases linearly with the increase of the total number of electrons and with a slope of -1 . As shown in Fig. 6(b), for all systems studied, the number of majority-spin electrons changes only slightly, but the number of minority electrons increases linearly with the total number of electrons and leads to the relation

TABLE V. Orbital-by-orbital contribution to the total magnetic moment μ (in Bohr magnetons) inside the various muffin-tin spheres of the 2Ni-Cu film.

	μ_s	μ_p	μ_d	μ_{tot}
Ni(S)	-0.003	-0.006	0.687	0.68
Ni(I)	-0.004	-0.010	0.482	0.47
Cu(I)	-0.005	-0.006	-0.006	-0.02
Cu(I-1)	0.000	-0.003	-0.001	-0.00
Cu(C)	-0.003	0.000	-0.007	-0.01

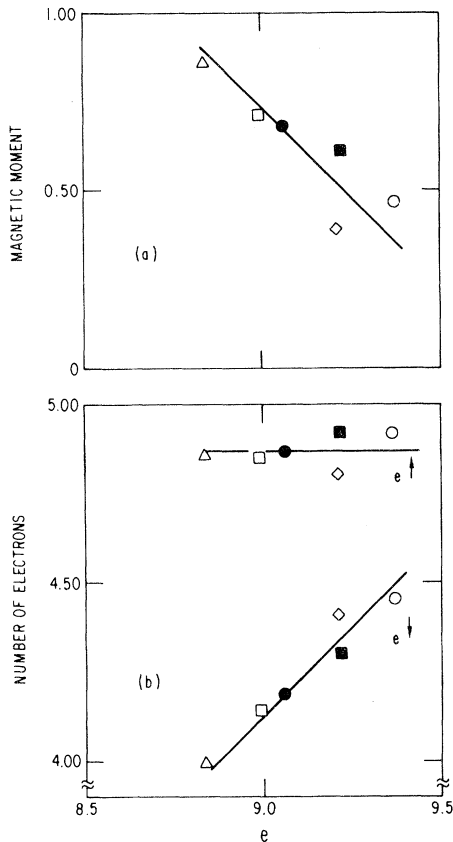


FIG. 6. Magnetic moment and the number of the spin-up and spin-down electrons vs the total number of electrons of the Ni atoms in various environments. \square and \circ are surface and interface Ni layers of the 2Ni-Cu film, \diamond is the Ni layer of the Ni-Cu film, \triangle is the isolated Ni monolayer (Ref. 16), and \bullet and \blacksquare are the surface and center layers of Ni(011) five-layer film (Ref. 12).

between the moment and total number of electrons shown in Fig. 6(a).

Examination of Fig. 6 leads to two observations which relate to the problem of surface magnetism. Firstly, the surface and interface affect the total number of electrons so that the surface atoms have fewer electrons, and the atoms in contact with the Cu substrate have more electrons due to the change of bonding. Secondly, the change in the total number of electrons arises almost completely from the minority-spin electrons and this leads to the decrease of the moment with an increase of the total number of electrons observed above. The majority-spin electrons are not involved because the shift of the $3d$ bands due to the change of bonding is not sufficiently great to lift the full majority band above the Fermi energy.

However, for some special regions in the 2D

Brillouin zone, such as the one close to \bar{M} in Fig. 3, the surface effect is more pronounced, and this lifts the \bar{M}_3 surface band above the bulk d -band edge and the Fermi energy and creates a pocket of majority holes. As pointed out in the case of clean Ni,¹⁰ this leads to a small decrease of the majority spin. As seen in Fig. 6(b), the number of majority electrons for all the layers on the surface is about 0.08 less than that of the interior layers. Usually, this effect is smaller than that caused by the change of bonding, but in some cases (for example, in a comparison of the bulk and Ni-Cu which have the same total number of electrons) it could become dominant (and cause the decrease of the moment of the Ni-Cu).

Changes of bonding on the splitting of the $3d$ majority and minority-spin bands are not independent; their splitting will change through the exchange correlation. For example, a shift of the minority band to lower binding energy will lead to an increase of the magnetic moment, which in turn causes the exchange splitting between the majority and minority band to increase. However, the exchange splitting (ΔE) is not the same for different states, as shown in Figs. 3(a) and 3(b). For the Ni-Cu film, the exchange splitting is 0.39 and 0.35 eV for $\bar{\Gamma}_4$ and $\bar{\Gamma}_5$, 0.28 and 0.37 eV for \bar{M}_1 and \bar{M}_3 , and 0.38 eV for \bar{X}_2 . An average exchange splitting, as measured from the layered projected DOS curve [Fig. 2(a) and 2(b)], is listed in Table VI. It is seen that the moment of the various layers is proportional to the exchange splitting. The ratio $\Delta E/\mu$, the so-called Stoner-Hubbard parameter, remains almost unchanged and also close to the value of the isolated monolayer and bulk Ni.¹⁶

Finally, as mentioned earlier, Fig. 6 reveals a correlation of the magnetic moment with the number of p -like electrons. At the surface this dehybridization of the s , p , and d electrons acts to increase the magnetic moment and is related to the d -band narrowing seen there. This dehybridization is also related to the simultaneous removal of p

TABLE VI. Exchange splitting (ΔE) of various Ni layers as determined from the upper edge of the layered projected DOS curves and the Stoner-Hubbard parameter $I (= \Delta E/\mu)$, where μ is the magnetic moment.

	ΔE (eV)	$\Delta E/\mu$ (eV/ μ_B)
Ni(S) of 2Ni-Cu	0.67	0.99
Ni(I) of 2Ni-Cu	0.52	1.11
Ni(S) of Ni-Cu	0.38	0.97

electrons from the muffin-tin (MT) spheres (where the d electrons are mainly localized) as they spill out into the vacuum region. It is not surprising that the number of p electrons in the MT region is correlated with the degree of dehybridization; in the free Ni atom, the p orbitals are completely *unoccupied*. There is a remarkable correlation between the total s and p charge of both spins, $q_s + q_p$ (μ_s and μ_p are essentially zero), and the magnetic moment. Since q_s is relatively unchanging ($\sim \pm 0.03$ electrons) this is, indeed, a correlation with q_p . In the unsupported Ni monolayers, where the first mechanism (the electrostatic-shift mechanism) is absent, this dehybridization accounts for the large increase of μ_d compared to the bulk value.¹² In all cases, the total charge in each vacuum region (there are two per slab) is equal (to within ~ 0.01 electrons) to the loss of p electrons from the MT spheres.

In the 2Ni-Cu slabs, other effects are seen, as mentioned above. Thus, charge transfer (about 0.1 electron from Table I) into the d bands of the interfacial Ni layer reduces the magnetic moment to $0.48\mu_B$ in this layer. Since this atom still has a coordination number of twelve, the dehybridization should not take place, as is also seen. By contrast, the surface Ni atoms of the 2Ni-Cu slab show some dehybridization, and could also have an upward electrostatic shift. Indeed, the Ni(*S*) atom does show a $3p_{3/2}$ core-level shift of 0.26 eV to reduced binding energy relative to the Ni(*I*) atom. Both of these effects are consistent with the increased moment of $0.69\mu_B$.

Recently, Tersoff and Falicov^{32(a)} have reported parametrized LCAO-type calculations using a real-space Green's-function formalism for up to four Ni overlayers on a semi-infinite Cu substrate.^{32(b)} In recent unpublished work^{32(b)} they find for Ni on Cu(001) results in good agreement with those obtained here.

VI. HYPERFINE FIELDS

From the calculated spin densities we may determine the Fermi contact contribution to the hyperfine field H_n at the nucleus.³³ This dominant part of the total hyperfine field consists of two parts: The well-known core-electron-polarization contribution and the contribution from the ($4s$) conduction electrons. The results are shown in Table VII. These are substantially larger than the (positive) contributions arising from unquenched orbital angular momentum or dipolar fields. The contribu-

tion from the (relativistic) $2p_{1/2}$ and $3p_{1/2}$ core electrons, which have a finite amplitude at the nucleus, are seen to be small—approximately 1% of the s -electron contributions.

For Ni, the negative core-polarization contribution dominates and is proportional to the local magnetic moment for both Ni(*S*) and Ni(*I*). This is seen in the constancy of the hyperfine field per magnetic moment, χ_{core} (-145 kG), which is surprisingly close to the free-atom Hartree-Fock result (~ -150 kG)—indicating that the $3d$ spin-magnetization density has about the same radial distribution in the film as in the free atom.³³ These results are also consistent with those for the bulk.³⁴ The contribution from the valence electrons is not simply proportional to the local electron-spin magnetic moment since it includes the addition of the rather slow decaying polarizations of the conduction-band electrons induced by many localized d moments.

For Cu, the core-polarization contribution to H_n is essentially zero; the calculated negative H_n at the Cu nuclei arises exclusively from the ($4s$) conduction electrons. This is an important result because its observation by NMR, which is relatively easy, would serve as strong evidence for the existence of a magnetic Ni overlayer. A similar effect has been seen at the Cu sites in the case of NiCu modulated structures.³⁵ (Note, however, that the magnitude of this contribution cannot serve as a measure of the magnetization of the overlayer because it is not proportional to H_n .) Further, as seen from Table VII, there is an oscillation of the Cu H_n with distance of the Cu layer from the magnetic Ni overlayers, which arises from the small Friedel-type oscillation of the spin density, driven by the Ruderman-Kittel-Kasuya-Yosida (RKKY) polarization mechanism. Although the exact behavior of this oscillation requires very high computational precision, its (expected) existence is shown clearly in our results.

Finally, the greater magnitude of the valence-electron contribution to H_n at Cu than at Ni, which appears unusual, requires analysis. In the free Ni atom, the closed-shell $4s$ electrons are polarized positively by direct exchange with the unpaired $3d$ electrons.³³ In the metal there is, in addition, another conduction-electron contribution to H_n which comes from the small net negatively unpaired $4s$ electrons (cf. Table V) which is of opposite sign to the direct exchange contribution from the larger number of paired $4s$ electrons (cf. Table II). Hence the contribution at the Ni sites in the overlayer is reduced to the small values given in

TABLE VII. Shell-by-shell contributions to the Fermi-contact hyperfine field for the different layers of the 2Ni-Cu system (in kG) and the hyperfine field per magnetic moment χ . Note that the free-atom χ value for Ni is ~ -150 (Ref. 33).

	Core contribution					Total	Valence (4s)	Hyperfine field	
	1s	2s	2p _{1/2}	3s	3p _{1/2}		contribution	H (kG)	χ core
Ni(S)	-8	-215	-2	125	1	-99	-21	-120	-146
Ni(I)	-7	-154	-1	93	1	-68	-23	-91	-145
Cu(I)	0	-1	0	1	0	0	-46	-46	
Cu(I-1)	1	-1	0	0	0	0	5	5	
Cu(C)	0	0	0	0	0	0	-32	-32	

Table VII. By contrast, in the case of the Cu layers, the only contribution to H_n comes from the negative conduction-electron spin density produced by the RKKY mechanism.

VII. CONCLUSION

We have reported detailed results of self-consistent spin-polarized LAPW energy-band studies for one and two layers of Ni on a Cu(001) substrate. We found that the Ni overlayers are not magnetically "dead." Surface and interface effects were found to be important and different in their effect on the magnetization, leading to a decrease in the moment of the interface Ni layers from the bulk value and to a small increase in the moment of the Ni surface-layer atoms. The reduced Ni interface moment was found to arise primarily from charge transfer onto these Ni sites from the Cu substrate. For the Ni surface atoms, a different mechanism was found to be operative: Here, the increase in moment for the Ni surface atoms turned out to be primarily due to the dehybridization of the p -like electrons from the d -band electrons with the loss of part of these p electrons. In a separate study, we found a similar effect for an unsupported Ni monolayer.¹²

Our work yields detailed information about spin magnetization and resulting direct and transferred Fermi-contact hyperfine fields H_n on the Ni and Cu sites. In the case of Ni, the (negative) core-polarization contribution dominates the conduction-electron contribution and is proportional to the local magnetic moment in both Ni(I) and Ni(S). For Cu, the core polarization is essentially zero and the calculated negative H_n arise almost entirely from the (4s) conduction electrons. These Cu fields are substantial in magnitude, and their measurement by NMR would provide strong evidence for the existence of a magnetically alive Ni overlayer on Cu(001).

ACKNOWLEDGMENTS

We are grateful to S. D. Bader and T. Jarlborg for helpful discussions and J. Tersoff and L. Falicov for an unpublished manuscript describing their work [Ref. 32(b)]. This work was supported by the National Science Foundation (Grant No. DMR77-23776), the Department of Energy, and by a grant from the Xerox Foundation.

*Permanent address: Institute of Physics, Academia Sinica, Beijing, People's Republic of China.

¹L. N. Liebermann, J. Clinton, D. M. Edwards, and J. Mathon, Phys. Rev. Lett. **25**, 232 (1970).

²U. Gradmann, J. Magn. Magn. Mater. **6**, 173 (1977).

³S. Eichner, C. Rau, and R. Sizmann, J. Magn. Magn. Mater. **6**, 204 (1977).

⁴M. Sato and K. Hirakawa, J. Phys. Soc. Jpn. **39**, 1467 (1975).

⁵G. Bergmann, Phys. Rev. Lett. **41**, 264 (1978).

⁶D. T. Pierce and H. C. Siegmann, Phys. Rev. B **9**, 4035 (1974).

⁷C. Rau, Bull. Amer. Phys. Soc. **25**, 234 (1980).

⁸P. Fulde, A. Luther, and R. E. Watson, Phys. Rev. B **8**, 440 (1973).

⁹K. Levin, A. Liebsch, and K. H. Benneman, Phys. Rev. B **7**, 3066 (1973).

¹⁰C. S. Wang and A. J. Freeman, Phys. Rev. B **21**, 4585 (1980).

¹¹O. Jepsen, J. Madsen, and O. K. Andersen, J. Magn. Magn. Mater. **15-18**, 867 (1980).

¹²H. Krakauer and A. J. Freeman, Bull. Amer. Phys. Soc. **26**, 356 (1981).

¹³H. J. Bauer, D. Blechschmidt, and M. V. Hellermann,

- Surf. Sci. 30, 701 (1972).
- ¹⁴D. S. Wang, A. J. Freeman, and H. Krakauer, J. Appl. Phys. 52, 2502 (1981).
- ¹⁵D. S. Wang, A. J. Freeman, and H. Krakauer, Bull. Amer. Phys. Soc. 26, 355 (1981).
- ¹⁶D. S. Wang, A. J. Freeman, and H. Krakauer, Phys. Rev. B 24, 1126 (1981).
- ¹⁷H. Krakauer, M. Posternak, and A. J. Freeman, Phys. Rev. B 19, 1706 (1979).
- ¹⁸M. Posternak, H. Krakauer, A. J. Freeman, and D. D. Koelling, Phys. Rev. B 21, 5601 (1980).
- ¹⁹V. von Barth and L. Hedin, J. Phys. C 5, 1629 (1972).
- ²⁰L. Hedin and B. I. Lundqvist, J. Phys. C 4, 2064 (1971).
- ²¹G. A. Haas and R. E. Thomas, J. Appl. Phys. 48, 86 (1977); G. G. Tibbetts, J. M. Burkstrand, and J. C. Tracy, Phys. Rev. B 15, 3652 (1977).
- ²²J. G. Gay, J. R. Smith, and F. J. Arlinghaus, Phys. Rev. Lett. 42, 332 (1979); Phys. Rev. B 21, 2201 (1980).
- ²³P. H. Citrin, G. K. Wertheim, and Y. Baer, Phys. Rev. Lett. 41, 1425 (1978).
- ²⁴J. A. Appelbaum and D. R. Hamann, Solid State Commun. 27, 881 (1978).
- ²⁵M. Mehta and C. S. Fadley, Phys. Rev. Lett. 39, 1569 (1977).
- ²⁶R. S. Williams, S. P. Kowalczyk, P. S. Wehner, G. Apai, J. Stöhr, and D. A. Shirley, J. Electron Spectrosc. Relat. Phenom. 12, 447 (1977).
- ²⁷C. S. Wang and J. Callaway, Phys. Rev. B 15, 298 (1977).
- ²⁸T. Jarlborg and A. J. Freeman, J. Magn. Magn. Mater. 22, 6 (1980).
- ²⁹In this paper the x and y coordinates are aligned with the square edges of the 2D square lattice of the (001) surface of a fcc crystal. They are rotated by 45° from the conventional 3D cubic unit cell. Here the $d_{x^2-y^2}$ state corresponds to the d_{xy} state in the usual 3D notation.
- ³⁰P. Heimann, J. Hermanson, H. Miosga, and H. Neddermeyer, Phys. Rev. B 20, 3059 (1979).
- ³¹Although their difference is small in the bulk, they are not degenerate, as misstated in Ref. 16.
- ³²J. Tersoff and L. M. Falicov, (a) Phys. Rev. B 24, 754 (1981), and (b) unpublished.
- ³³R. E. Watson and A. J. Freeman, Phys. Rev. 123, 2027 (1961).
- ³⁴A. J. Freeman and R. E. Watson, in *Magnetism*, edited by G. Rado and H. Suhl (Academic, New York, 1964), Vol. IIA, p. 167.
- ³⁵T. Jarlborg and A. J. Freeman, Phys. Rev. Lett. 45, 653 (1980).